Published in final edited form as:
Biochem Soc Trans. 2011 October ; 39(5): 1131–1135. doi:10.1042/BST0391131.

Distinct and redundant roles of the non-muscle myosin II isoforms and functional domains

Aibing Wang, **Xuefei Ma**, **Mary Anne Conti**, and **Robert S. Adelstein**[1]
Laboratory of Molecular Cardiology, National Heart, Lung, and Blood Institute, National Institutes of Health, Bethesda, MD 20892-1583, U.S.A

Abstract

We propose that the *in vivo* functions of NM II (non-muscle myosin II) can be divided between those that depend on the N-terminal globular motor domain and those less dependent on motor activity but more dependent on the C-terminal domain. The former, being more dependent on the kinetic properties of NM II to translocate actin filaments, are less amenable to substitution by different NM II isoforms, whereas the *in vivo* functions of the latter, which involve the structural properties of NM II to cross-link actin filaments, are more amenable to substitution. In light of this hypothesis, we examine the ability of NM II-A, as well as a motor-compromised form of NM II-B, to replace NM II-B and rescue neuroepithelial cell–cell adhesion defects and hydrocephalus in the brain of NM II-B-depleted mice. We also examine the ability of NM II-B as well as chimaeric forms of NM II (II-A head and II-B tail and vice versa) to substitute for NM II-A in cell–cell adhesions in II-A-ablated mice. However, we also show that certain functions, such as neuronal cell migration in the developing brain and vascularization of the mouse embryo and placenta, specifically require NM II-B and II-A respectively.

Keywords

cell–cell adhesion; cell migration; hydrocephalus; myosin; non-muscle myosin II

Introduction

The myosin II molecule is distinguished by a very asymmetric shape with a globular head domain at the N-terminal end followed by an α-helical coiled-coil rod domain that terminates in a non-helical tail. This asymmetry is reflected in myosin's functional activity: the N-terminal motor domain binds to actin and the contraction is powered by actin-activated MgATPase activity that is regulated by phosphorylation of the 20 kDa regulatory light chain. The C-terminal α-helical rod domain has the capability to form bipolar filaments, thereby cross-linking actin filaments and exerting tension. Our laboratory has been studying the function of mammalian NM II (non-muscle myosin II), concentrating in particular on the role of NM II *in vivo*.

In mammals, there are three genes (*Myh9*, *Myh10* and *Myh14*) that encode the NMHC (non-muscle myosin heavy chain; 230 kDa) proteins, named NMHC II-A, II-B and II-C [1,2]. The NMHCs exhibit 60–80% identity at the amino acid level, but have sufficient differences in sequence to allow generation of isoform-specific antibodies [3]. A myosin molecule consists of a dimer of the heavy chains and two pairs of light chains, which appear

[1]To whom correspondence should be addressed: adelster@mail.nih.gov.

to be common to each of the three isoforms. We refer to the hexameric isoforms as NM II-A, NM II-B and NM II-C. One pair of light chains [RMLC (regulatory myosin light chain), 20 kDa] regulates the actin-activated MgATPase activity and also plays a role in myosin filament formation by reversible phosphorylation of specific serine (Ser^{19}) and threonine (Thr^{18}) residues. The second pair of light chains [EMLC (essential myosin light chain), 17 kDa] helps to stabilize the heavy chain conformation and structure.

The question arises, with three different genes located on three different chromosomes, as to how much redundancy in function exists among the isoforms and whether the ability of one isoform to substitute for another can be traced to the two major domains of the molecule: the globular head and the filamentous tail. In the present paper, we explore the following hypothesis: the NM II molecule has two distinctive domains that govern different functions. (i) A globular N-terminal head or motor domain that is responsible for translocation of actin filaments and depends on the actin-activated MgATPase activity. This function is dependent on the motor activity of the NM II isoform and because of significant differences in both the rate of MgATP hydrolysis and the duty ratio (the amount of time myosin is bound to actin during the contractile cycle) among the isoforms, this function is not amenable to isoform substitution. (ii) An α-helical C-terminal tail of the molecule that governs bipolar filament formation. These filaments play a role in cell–cell adhesion during which NM II exerts tension on actin for long periods of time. These functions are mostly independent of the enzymatic activity of the motor and are amenable to substitution by other NM II isoforms. Below we review some of the experiments that were performed to address the hypothesis.

NM II-B replacement *in vivo* during mouse brain development

Germline ablation of NM II-B results in defects in both the heart and brain [4,5]. The brain abnormalities include hydrocephalus, the abnormal migration of distinct groups of neuronal cells, including the facial neurons that end up in the fourth ventricle, as well as the abnormal migration of the pontine neurons and the granular cells of the cerebellum [6]. In an effort to generate a putative mouse model for a human disease, we introduced a point mutation (R709C) into exon 17 of *Myh10*. We chose this mutation because a homologous mutation in humans in NM II-A and NM II-C was found to cause disease [7–9]. We had previously characterized a HMM (heavy meromyosin) fragment with this mutation and shown that the mutant HMM had an actin-activated MgATPase activity that was decreased by 67% and, although it could bind to actin filaments and be released by ATP, it could not translocate actin filaments in an *in vitro* motility assay [10]. Despite these changes in the properties of the mutant myosin, we found that replacement of wild-type NM II-B by the mutant NM II-B^{R709C}, using homologous recombination, resulted in mice that showed no evidence of hydrocephalus [11]. Analysis of the cells lining the spinal canal in II-B-ablated and II-B-hypomorphic mice pinpointed the cause of the hydrocephalus as a loss of cell–cell adhesion in the neuroepithelial cells lining the spinal canal. NM II-B (and actin) co-localized with N-cadherin and β-catenin in an adhesion complex at the periphery of the cells [11]. Absence of NM II-B, the only NM II expressed in these cells, resulted in a loss of the integrity of cell–cell adhesions of the cells lining the canal and permitted the underlying neuroepithelial cells to invade into the spinal canal, thereby obstructing the flow of cerebral spinal fluid. These experiments also suggested that the motor activity of NM II, which was diminished in the mutant myosin, was not required for cell–cell adhesion and was consistent with the idea that the scaffolding properties of the myosin molecule, which require binding to actin, play an important role in cell adhesion. This idea was supported further by our finding that the mutant myosin localized to the cell boundaries in the same manner as the wild-type NM II-B [11].

We tested further the hypothesis by generating a mouse in which NM II-B was replaced by NM II-A, by inserting cDNA encoding NMHC II-A into the first exon of *Myh10*, thereby

ablating the endogenous NMHC II-B and placing exogenous NMHC II-A under control of the II-B promoter [12]. These mice also showed no evidence of hydrocephalus, and immunofluorescence microscopy showed that the neuroepithelial cells lining the spinal canal were all intact, but with NM II-A localized to the cell–cell boundaries in place of NM II-B. In contrast, neither mutant myosin nor exogenous NM II-A were able to rescue the pontine and facial neurons defects in cell migration found in the II-B-ablated mice. This could be attributed to the marked difference between the motor properties of NM II-A and II-B (V_{max} 0.45 s^{-1} for II-A and 0.17 s^{-1} for II-B), as well as the prolonged duty ratio of II-B compared with II-A [10,13,14]; and supported the idea that these properties are less amenable to substation than the structural ones.

NM II-A replacement during mouse development

Germline ablation of NM II-A provided another opportunity to test the hypothesis. The NM II-A-ablated mice died by E6.5 (where E is embryonic day) before gastrulation and demonstrated two major (not unrelated) abnormalities [15]: a decrease in cell–cell adhesion and a failure to develop a functional visceral endoderm (Figure 1). The demise of these mice before gastrulation could be explained by the latter finding, since a normally functioning visceral endoderm is required for continued development. As shown in Figure 1(B), the mutant visceral endoderm is disorganized and mislocalizes E-cadherin (and β-catenin, results not shown) at the cell–cell boundaries, in contrast with the control embryo (Figure 1A). Immunostaining of the E6.5 control embryo revealed that all of the cells of the embryo as well as the extra embryonic tissue, which includes the visceral endoderm, contain NM II-A and II-B, with the exception of the visceral endoderm that lacks NM II-B [15]. At this stage of development, the mouse embryo lacks NM II-C. The absence of NM II-B from the visceral endoderm could explain why the visceral endoderm failed to function in the II-A-ablated mice. It also raised the question as to whether NM II-A was specifically required for normal function or whether NM II-B could substitute for NM II-A during early embryonic development and specifically restore a normal functioning visceral endoderm and allow the embryo to gastrulate. Importantly it permitted a more in-depth analysis of our hypothesis concerning isoform substitution with respect to the two domains (globular head and filamentous tail) of the NM II molecule. We generated the following mouse lines: a line in which we used cDNA encoding NMHC II-B to ablate NMHC II-A, and placed the exogenous NMHC II-B under control of the endogenous NMHC II-A promoter (A^{b*}/A^{b*} mice); a line in which we introduced a chimaeric cDNA (II-A/II-B), with the II-A head domain fused to the II-B tail domain, into the same Myh9 locus (A^{ab}/A^{ba} mice) and likewise introduced a chimaeric II-B/II-A into the same locus (A^{ba}/A^{ba} mice) [16]. As evidence that the genetic manipulations required for these experiments did not affect overall expression, we also generated control mice in which mCherry was fused to NMHC II-A cDNA and inserted into the same *Myh9* locus. These latter mice produced litters at the expected Mendelian ratios, had a normal lifespan and were normal with respect to phenotype; although there was evidence for aggregation of mCherry–NM II in some of the cells [16].

All three exogenous NM IIs were able to replace endogenous NM II-A during early mouse development, allowing for formation of a normal visceral endoderm and permitting the mutant mice to gastrulate and to initiate organ development [16]. Figure 1 shows immunofluorescence staining of E6.5 embryos for NM II-A, II-B and the cell adhesion protein E-cadherin. Note the absence of NM II-B from the cell–cell borders of the visceral endoderm in wild-type embryos (Figure 1I, arrows) and the absence of NM II-A from the same location in the mutant mouse (Figure 1F, arrows) and its replacement by NM II-B (Figure 1J, arrow). All three lines of mutant mice are able to initiate organ development, but, owing to abnormalities in the placenta, the A^{b*}/A^{b*} (Figure 2B) and the A^{ba}/A^{ba} (not shown) mice die at E9.5–10.5. The cause of death is the failure in vascular development in

the mutant mice that can be seen by comparing the mutant (Figures 2B and 2D) and the wild-type (Figures 2A and 2C), whereas the labyrinthine layer of the A^{+}/A^{+} placenta demonstrates a network of fetal capillaries and maternal blood sinuses, the former containing nucleated red cells (Figure 2C, green arrow) and the latter mature red cells (Figure 2C, yellow arrow). The mutant A^{ba}/A^{ba} mice show that, owing to a compromised vasculature, the two pools of red cells remain separated (Figure 2D). This is also demonstrated by staining the placenta vasculature with CD34 (green), a marker for endothelial cells. Figure 2(F) shows that very few cells have invaded the labyrinthine layer, in contrast with the A^{+}/A^{+} embryo (Figure 2E). Interestingly, the mutant A^{ab}/A^{ab} mice, which survive until E11.5–12.5, in contrast with the two other mutant lines, show less severe vascular defects with more CD34+ cells entering the labyrinthine layer than A^{ba}/A^{ba} and A^{b*}/A^{b*} mice [16]. We interpret this to mean that NM II-A, unlike NM II-B plays an irreplaceable role during placenta development, and that the presence of II-A motor domain partially rescues the defect in vessel invasion. Consistent with this is the finding that B^{-}/B^{-} mice at this stage of development (E11.5) show normal placental development [16].

Cell migration defects in the mutant mice

The abnormal invasion of the placenta by blood vessels that we found in the mutant mice when II-A is replaced prompted us to study cell migration using primary cultures of fibroblasts derived from the three mutant cell lines. We made use of both a wound-healing assay to study speed of migration and a transwell assay to study perseverance of migration. Interestingly both the A^{b*}/A^{b*} and A^{ba}/A^{ba} fibroblasts migrate more rapidly than do the A^{+}/A^{+} and A^{ab}/A^{ab} ones [16]. The faster migration is similar to that previously found for II-A-ablated cell migration [17] and suggests that the II-A head domain of the A^{ab}/A^{ab} mice is sufficient to restore the wild-type speed of migration to the mutant cells. In contrast, fewer cells from all three mutant mouse lines were found to migrate through the membrane into the lower chamber in the transwell assay compared with wild-type during the same period of time, indicating that all the mutant lines have defects in directed cell migration [16]. These results show that the absence of the II-A in either the head or rod domains (or both) causes abnormalities in the speed and persistence of migration, showing the important but separate contribution of the individual domains to cell migration.

To probe further the mechanism underlying cell migration in the mutant cells, we compared the actin stress fibres and focal adhesions between wild-type and mutant mouse embryo fibroblasts [16]. We found that the stress fibres of the wild-type mouse cells were better organized and more often aligned with the direction of migration than the thinner, more disorganized stress fibres found in the mutant fibroblasts. In addition, the mutant fibroblasts have fewer and smaller focal adhesions compared with wild-type cells. Immunoblot analysis of A^{b*}/A^{b*} and A^{+}/A^{+} fibroblasts showed that there was no change in the content of paxillin and vinculin between the two lines, but the wild-type cells contained phospho-Tyr^{118} paxillin that was missing or decreased in the mutant cells. Phosphorylated paxillin is required for focal adhesion maturation, and its absence could help explain the lack of persistence in fibroblast migration. Importantly, introducing wild-type NM II-A into the A^{b*}/A^{b*} cells increased the number of focal adhesions, showing that the loss of focal adhesions was due to the loss of NM II-A, despite its replacement by NM II-B. We are presently planning more experiments to decipher the exact role of NM II in focal adhesion formation particularly during vascular development.

Summary

Table 1 summarizes the mouse models discussed above and includes a few related lines that have been generated. It is of note, but not surprise, that embryonic defects often occur in

knockout mice in tissues that contain a single or predominant amount of a single isoform, for example, the heart and neuronal cells in the case of II-B and the visceral endoderm in the case of NM II-A. Although we found no obvious defects in NM II-C-ablated mice and although the content of NM II-C in cardiac myocytes is considerably less than NM II-B, the ablation of both NM II-C and II-B led to a significantly more severe phenotype with respect to karyokinesis than NM II-B alone [18]. These findings, along with the results from hypomorphic mice, point to the importance of the total content of NM II in many tissues. Thus total content along with a distinct motor domain appears to be required for certain functions of NM II, whereas the ability of all three NM II isoforms to form bipolar filaments and exert tension suffices for other functions.

Acknowledgments

Funding

This work was funded by the National Heart, Lung, and Blood Institute/National Institutes of Health, Division of Intramural Research.

Abbreviations used

E	embryonic day
HMM	heavy meromyosin
NM II	non-muscle myosin II
NMHC	non-muscle myosin heavy chain

References

1. Berg JS, Powell BC, Cheney RE. A millennial myosin census. Mol Biol Cell. 2001; 12:780–794. [PubMed: 11294886]
2. Golomb E, Ma X, Jana SS, Preston YA, Kawamoto S, Shoham NG, Goldin E, Conti MA, Sellers JR, Adelstein RS. Identification and characterization of nonmuscle myosin II-C, a new member of the myosin II family. J Biol Chem. 2004; 279:2800–2808. [PubMed: 14594953]
3. Conti, MA.; Kawamoto, S.; Adelstein, RS. Non-muscle myosin II. In: Coluccio, LM., editor. Myosins: A Superfamily of Molecular Motors. Springer; Watertown: 2008. p. 223-264.
4. Tullio AN, Accili D, Ferrans VJ, Yu ZX, Takeda K, Grinberg A, Westphal H, Preston YA, Adelstein RS. Nonmuscle myosin II-B is required for normal development of the mouse heart. Proc Natl Acad Sci USA. 1997; 94:12407–12412. [PubMed: 9356462]
5. Tullio AN, Bridgman PC, Tresser NJ, Chan CC, Conti MA, Adelstein RS, Hara Y. Structural abnormalities develop in the brain after ablation of the gene encoding nonmuscle myosin II-B heavy chain. J Comp Neurol. 2001; 433:62–74. [PubMed: 11283949]
6. Ma X, Kawamoto S, Hara Y, Adelstein RS. A point mutation in the motor domain of nonmuscle myosin II-B impairs migration of distinct groups of neurons. Mol Biol Cell. 2004; 15:2568–2579. [PubMed: 15034141]
7. Burt RA, Joseph JE, Milliken S, Collinge JE, Kile BT. Description of a novel mutation leading to MYH9-related disease. Thromb Res. 2008; 122:861–863. [PubMed: 18676005]
8. Donaudy F, Snoeckx R, Pfister M, Zenner HP, Blin N, Di SM, Ferrara A, Lanzara C, Ficarella R, Declau F, et al. Nonmuscle myosin heavy-chain gene MYH14 is expressed in cochlea and mutated in patients affected by autosomal dominant hearing impairment (DFNA4). Am J Hum Genet. 2004; 74:770–776. [PubMed: 15015131]
9. Seri M, Pecci A, Di BF, Cusano R, Savino M, Panza E, Nigro A, Noris P, Gangarossa S, Rocca B, et al. MYH9-related disease: May–Hegglin anomaly, Sebastian syndrome, Fechtner syndrome, and Epstein syndrome are not distinct entities but represent a variable expression of a single illness. Medicine. 2003; 82:203–215. [PubMed: 12792306]

10. Kim KY, Kovacs M, Kawamoto S, Sellers JR, Adelstein RS. Disease-associated mutations and alternative splicing alter the enzymatic and motile activity of nonmuscle myosins II-B and II-C. J Biol Chem. 2005; 280:22769–22775. [PubMed: 15845534]
11. Ma X, Bao J, Adelstein RS. Loss of cell adhesion causes hydrocephalus in nonmuscle myosin II-B-ablated and mutated mice. Mol Biol Cell. 2007; 18:2305–2312. [PubMed: 17429076]
12. Bao J, Ma X, Liu C, Adelstein RS. Replacement of nonmuscle myosin II-B with II-A rescues brain but not cardiac defects in mice. J Biol Chem. 2007; 282:22102–22111. [PubMed: 17519229]
13. Kovacs M, Toth J, Nyitray L, Sellers JR. Two-headed binding of the unphosphorylated nonmuscle heavy meromyosin·ADP complex to actin. Biochemistry. 2004; 43:4219–4226. [PubMed: 15065866]
14. Kovacs M, Wang F, Hu A, Zhang Y, Sellers JR. Functional divergence of human cytoplasmic myosin II: kinetic characterization of the non-muscle IIA isoform. J Biol Chem. 2003; 278:38132–38140. [PubMed: 12847096]
15. Conti MA, Even-Ram S, Liu C, Yamada KM, Adelstein RS. Defects in cell adhesion and the visceral endoderm following ablation of nonmuscle myosin heavy chain II-A in mice. J Biol Chem. 2004; 279:41263–41266. [PubMed: 15292239]
16. Wang A, Ma X, Conti MA, Liu C, Kawamoto S, Adelstein RS. Nonmuscle myosin II isoform and domain specificity during early mouse development. Proc Natl Acad Sci USA. 2010; 107:14645–14650. [PubMed: 20679233]
17. Even-Ram S, Doyle AD, Conti MA, Matsumoto K, Adelstein RS, Yamada KM. Myosin IIA regulates cell motility and actomyosin–microtubule crosstalk. Nat Cell Biol. 2007; 9:299–309. [PubMed: 17310241]
18. Ma X, Jana SS, Conti MA, Kawamoto S, Claycomb WC, Adelstein RS. Ablation of nonmuscle myosin II-B and II-C reveals a role for nonmuscle myosin II in cardiac myocyte karyokinesis. Mol Biol Cell. 2010; 21:3952–3962. [PubMed: 20861308]
19. Takeda K, Kishi H, Ma X, Yu ZX, Adelstein RS. Ablation and mutation of nonmuscle myosin heavy chain II-B results in a defect in cardiac myocyte cytokinesis. Circ Res. 2003; 93:330–337. [PubMed: 12893741]

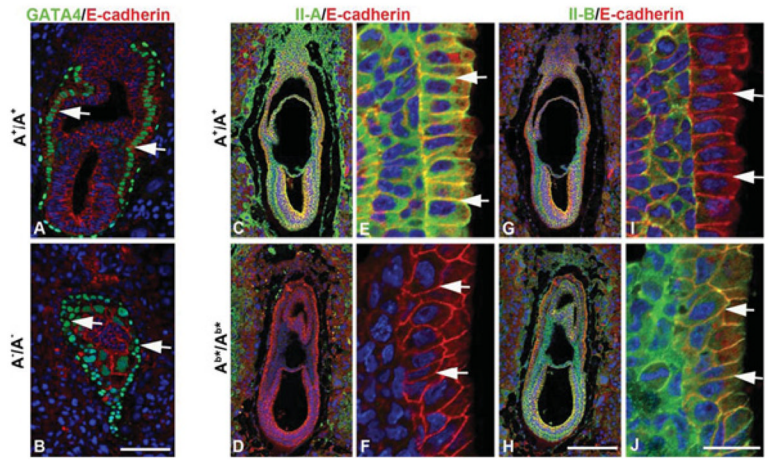

Figure 1. A^{b*}/A^{b*} embryos exhibit normal visceral endoderm at E6.5

E6.5 A^{+}/A^{+} (**A**) and A^{-}/A^{-} (**B**) embryo sections are stained with antibodies to E-cadherin (red) and GATA4 (green), a specific marker of visceral endoderm. Sections from E6.5 A^{+}/A^{+} (**C**, **E**, **G** and **I**) and A^{b*}/A^{b*} (**D**, **F**, **H** and **J**) embryos are stained with antibodies detecting E-cadherin (red) and NM II-A (green) or NM II-B (green). (**E**, **F**, **I** and **J**) Enlarged from (**C**, **D**, **G** and **H**). There is no difference in the morphology, including embryo size and cell-layer organization, between A^{+}/A^{+} and A^{b*}/A^{b*} embryos. Of note, the wild-type visceral endoderm expresses NM II-A (**E**, arrows) but lacks II-B (**I**, arrows), whereas A^{b*}/A^{b*} embryos lack NM II-A (**F**, arrows) and instead express II-B at the cell boundaries of the visceral endoderm (**J**, arrows). DAPI (4′,6-diamidino-2-phenylindole; blue) stains the nuclei. Scale bars, 100 μm in (**B**) and (**H**); 20 μm in (**J**). Modified from [16] with permission.

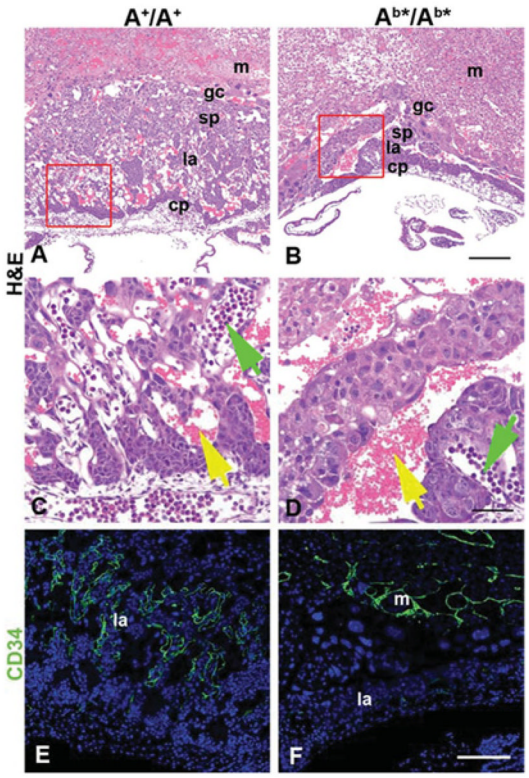

Figure 2. Placenta defects in E10.5 A^{b*}/A^{b*} mice

(**A** and **B**) H&E (haematoxylin and eosin) stained sections of A^{+}/A^{+} and (**B**) A^{b*}/A^{b*} placentas. At E10.5, A^{b*}/A^{b*} placentas are markedly thinner compared with the A^{+}/A^{+} and lack fetal vessels in the labyrinthine layer. (**C** and **D**) Magnified from the red boxes in (**A**) and (**B**). In (**C**), fetal blood vessels with nucleated erythrocytes (green arrow) invade and mix with maternal blood vessels (yellow arrow). In (**D**), embryonic blood vessels (green arrow) do not invade but remain on the edge of the labyrinthine layer. (**E** and **F**) Endothelial cell distribution in A^{+}/A^{+} and A^{b*}/A^{b*} placentas is visualized with a CD34 antibody (green). Almost no endothelial cells are seen in the labyrinthine layer of the A^{b*}/A^{b*} placenta when compared with the A^{+}/A^{+} placenta. Orientation in all panels has the maternal side towards the top and the fetal side towards the bottom. Abbreviations: cp, chorionic plate; gc, giant cells; la, labyrinthine layer; m, maternal tissue; sp, spongiotrophoblast layer. DAPI stains nuclei in (**E**) and (**F**). Scale bars, 200 μm in (**B**) and (**F**); 50 μm in (**D**). Reprinted from [16] with permission.

Table 1

Summary of phenotypes of genetically modified mice

Genotype	Lethality	Phenotype
A^{-}/A^{-}	E6.5	Defects in cell–cell adhesion and visceral endoderm formation. No gastrulation [15]
B^{-}/B^{-}	E14.5	Defects in heart (VSD and DORV) and brain (hydrocephalus and neuronal migration defects) [4,5]
C^{-}/C^{-}	Adult	No obvious abnormalities [18]
B^{-} C^{-}/B^{-} C^{-}	E14.5	Defects in heart and brain as B^{-}/B^{-} mice with major abnormalities in cardiac myocyte karyokinesis [18]
A^{b*}/A^{b*} hNMHC II-B under control of II-A promoter	E9.5–10.5	Visceral endoderm cell–cell adhesion defect rescued, embryos undergo gastrulation. Defects in placental development due to lack of endothelial cell migration [16]
B^{a*}/B^{a*} hNMHC II-A under control of II-B promoter	E14.5	Hydrocephalus rescued by restoring neuroepithelial cell–cell adhesion. Neuronal migration and heart defects not rescued [12]
A^{ba}/A^{ba} hNMHC II-BA under control of II-A promoter	E9.5–10.5	Cell–cell adhesion rescued, embryos gastrulate. Defects in placental development due to lack of endothelial cell migration [16]
A^{ab}/A^{ab} hNMHC II-AB under control of II-A promoter	E11.5–12.5	Cell–cell adhesion rescued, embryos gastrulate. Defects in placental development due to lack of endothelial cell migration. The NMHC II-A N-terminus, which contains the II-A motor domain, permits longer survival compared with the II-B N-terminus [16]
B^{CN}/B^{CN} lower expression of R709C mutant II-B	E14.5	Defects in heart (VSD and DORV) and brain (hydrocephalus and neuronal migration defects) [6,19]
B^{C}/B^{C} wild-type levels of R709C mutant II-B	E14.5	Hydrocephalus rescued by restoring neuroepithelial cell–cell adhesion. Neuronal migration and heart defects (VSD and DORV) not rescued [11]

DORV, doublet out right ventricle; VSD, ventricular septal defect.